Stability analysis of oscillators driven with multi-harmonic sources

Elena Fernández, Franco Ramírez, Almudena Suárez, Sergio Sancho
Dpt. Ingeniería de Comunicaciones.
Univeristy of Cantabria
Santander, Spain

***Abstract* — An investigation of the synchronization behavior of oscillators driven with multi-harmonic sources is presented. The occurrence of ultra-subharmonic synchronization is demonstrated, which gives rise to a multi-resonance behavior versus the fundamental input frequency. When this frequency decreases, instabilities arise in the low amplitude intervals of the multi-resonance curve, and both flip and Hopf bifurcation may delimit the stable synchronization intervals. The study provides a generalization of the theory of fundamentally locked oscillators to the case of oscillators driven with multi-harmonic signals. It is illustrated through application to an oscillator at 5.7 GHz.**

***Keywords* — Injection locking, switched oscillators, stability, bifurcation.**

I. Introduction

Pulsed-injection locked oscillators can be used for fast frequency hopping and for the generation of ultrawideband signals in radar and communication applications [1-2]. The oscillation is turned on and off with a pulse signal and the circuit is designed so as to enable the injection-locking of the oscillation to a harmonic component of the pulse frequency. As shown in [1-2], the pulse-injection locked oscillator can have the advantage of short transient behavior and lower phase noise. The model presented for the prediction of the locking range is based on Adler's equation and therefore on a linearization about the free-running steady-state oscillation. In [3], the nonlinear behavior of the whole circuit with respect to the input pulse is shown, which would prevent the use of linearized approaches. The work [3] presents a simplified mathematical model of the pulse-injection oscillator, which demonstrates the phase relationship between the oscillation and the input pulse. However, no in-depth study of the synchronized response versus the pulse frequency is carried out, which would be essential to understand the differences with respect to ordinary injection-locked oscillators at the fundamental frequency. Furthermore, no detailed analysis of the instability phenomena, delimiting the synchronization bands, has been carried out.

The works [1-3] are examples of oscillator synchronization with input signals different from a sinusoid. The objective of this paper is to present a detailed analysis of the oscillator behavior when driven with a multi-harmonic signal. In particular, a square waveform of low duty cycle will be considered, able to turn the oscillation on and off. A multi-resonance response is demonstrated, with theoretical insight into the possible instability phenomena when varying the fundamental frequency of the input source. The study provides a generalization of the theory of sinusoidal injection-locked oscillators to the case of oscillators driven with multi-harmonic sources. It will be illustrated with a bipolar-based pulse-injection oscillator at 5.7 GHz.

II. Multi-Resonance Behavior

For the analysis of injection locking with multi-harmonic sources, a Fourier-series representation of a square waveform will be considered $p(t)=\sum_{k=-N}^{N} P_k e^{jk\omega_p t}$, with ω_p being the fundamental frequency, called here the pulse frequency. Initially the case of a cubic nonlinearity oscillator, with a parallel RLC resonator is studied. The voltage source p(t), in series between the nonlinearity and the resonator, turns the oscillation on and off. The free-running oscillation frequency ω_0 is 1.586 GHz and N = 14 harmonic terms are considered in p(t). Fig. 1 presents the solution curve versus ω_p. The maximum of the periodic waveform (obtained for a specific time value) is traced versus ω_p. The curve has been obtained with harmonic balance (HB) with a high number of harmonic terms. As shown in [3] in pulse-injection locked oscillators the synchronized solution does not generally coexist with any non-oscillatory (trivial) solution. This is different from the case of sinusoidally injection-locked oscillators with small injection power. Thus, there will be no need for complementary techniques, such as the one based on the use of auxiliary generators [4]. Though the HB analysis is computationally costly, it can have advantages for the understanding of the global behavior of the circuit.

The pattern of the solution curve in Fig. 1 shows an ultra-subharmonic synchronization phenomenon [5], with multiple resonances occurring about the frequencies where ω_p and ω_0 fulfill a rational relationship: $r\omega_p = m\omega_0$, for $r,m \in \mathbb{Z}$. As ω_p decreases, the resonances become narrower, due to the need of a much higher r to fulfill the rational relationship. The phenomenon can be related to the Arnold tongues in sinusoidally synchronized oscillators, described in [5]. However, there are essential differences. In a sinusoidal

oscillator only the major tongues at ω_0, $\omega_0/2$, $\omega_0/3$, $2\omega_0$, $3\omega_o$ are relevant, unless a specific design to favor a particular rational relationship is carried out. This is shown clearly in the analysis of Fig. 1b, which presents the oscillator response versus the input frequency for N = 1,2,3 and N = 14. As shown in the figure, in the sinusoidal case (N = 1) resonances are obtained about the frequencies ω_0/r with r = 1, r = 2 and r = 3. As the number of input harmonic terms increases, the subharmonic resonances become more pronounced and ultra-subharmonic resonances arise in the system. This will enable the desired synchronization for high ratio between the oscillation frequency ω_0 and ω_p.

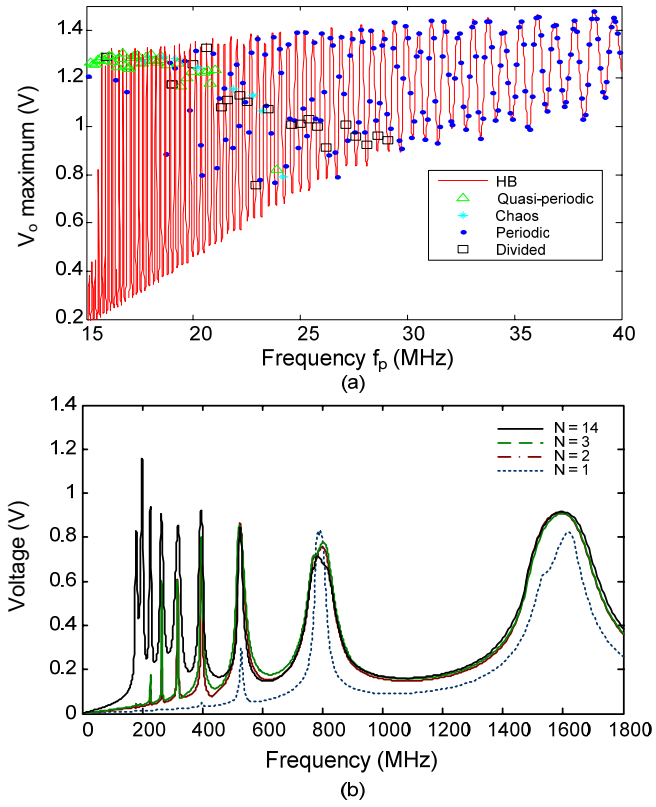

Fig. 1 Multi-resonance behavior at the input frequencies fulfilling $r\omega_p = m\omega_0$. (a) HB analysis for N = 14, with time-domain results superimposed. (b) HB analysis for different number of harmonic terms.

In order to understand the behavior in Fig. 1a, a simple mathematical model will be considered. Using a state form representation of the system, the circuit equations can be written:

$$\dot{\bar{x}} + \bar{f}(\bar{x}, p) = \bar{0} \qquad (1)$$

Where p(t) is the multi-harmonic input signal. The nonlinear function $\bar{f}(\bar{x}, p)$ can be expanded in power series as:

$$\bar{f}(\bar{x}, p) = \bar{f}(\bar{x}, 0) + \sum_{i=1}^{M} \bar{C}_i(\bar{x}) p(t)^i, \quad \bar{C}_i(\bar{x}) = \frac{1}{i!} \frac{\partial^i \bar{f}(\bar{x}, 0)}{\partial p^i} \qquad (2)$$

Expanding each term $p(t)^i$ using the Fourier series and rearranging the terms associated to the same frequencies:

$$\bar{f}(\bar{x}, p) = \bar{f}(\bar{x}, 0) + \sum_{r=-MN}^{MN} \bar{g}_r(\bar{x}, \bar{P}) U_r(\bar{P}) e^{j(r\omega_p t + \varphi_r)} = \\ = \bar{f}(\bar{x}, 0) + \sum_{r=-MN}^{MN} \bar{g}_r(\bar{x}, \bar{P}) u_r(t), \; u_r(t) = U_r(\bar{P}) e^{j(r\omega_p t + \varphi_r)} \qquad (3)$$

where MN is the order of the nonlinearity and $\bar{P}$ is the vector of harmonic components in p(t). The nonlinear function expands the spectrum of p(t) and introduces in the circuit 2MN + 1 single-tone equivalent sources $u_r(t)$. Each source $u_r(t)$ contains the frequency $r\omega_p$ and is modulated by the vector transfer function $\bar{g}_r(\bar{x}, \bar{P})$. In the case of small amplitude sources, the superposition principle can be applied. Then, for each source $u_r(t)$ we analyze the system:

$$\dot{\bar{x}} + \bar{f}(\bar{x}, 0) + \bar{g}_r(\bar{x}, \bar{P}) u_r(t) = \bar{0} \qquad (4)$$

If there exists an integer value $m > 0$ such that $\Delta\omega = r\omega_p - m\omega_0$ is small enough, then the oscillator gets synchronized to the source $u_r(t)$. The oscillation frequency moves from ω_0 to the value $\omega_0' = \omega_0 + \Delta\omega / m$. In that case, using the frequency ω_0' as fundamental, the system (4) can be translated to the frequency domain as:

$$\bar{H}\left[\bar{V}_0 + \Delta\bar{V}, \bar{\phi}_0 + \Delta\bar{\phi}, \omega_0 + \Delta\omega / m\right] + \bar{G}_r^m U_r e^{j\varphi_r} = \bar{0} \qquad (5)$$

where $\bar{H}$ is the vector function which translates the function $\bar{h}(\bar{x}, \dot{\bar{x}}) = \dot{\bar{x}} + \bar{f}(\bar{x}, 0)$ in (4), $\bar{V}_0$, $\bar{\phi}_0$ are the vectors containing the amplitude and phase of the harmonic components of $\bar{x}$ and $\bar{G}_r^m$ is the column of the Toeplitz matrix of the harmonic components of $\bar{g}_r(\bar{x}, \bar{P})$ associated to the m^{th} frequency component. For low $u_r(t)$, system (5) can be expanded in a first-order Taylor series as:

$$H_V \Delta\bar{V} + H_\phi \Delta\bar{\phi} + \bar{H}_\omega (r\omega_p / m - \omega_0) + \bar{G}_r^m U_r e^{j\varphi_r} = \bar{0} \qquad (6)$$

where H_V , H_ϕ and $\bar{H}_\omega$ are respectively the derivatives of the vector function $\bar{H}$ with respect to the amplitudes, phases and fundamental frequency. Varying the phase φ_r, a closed curve would be obtained in the $(\Delta V_{ik}, \omega_p)$ space, centered about $\omega_p = m\,\omega_0/r$ and providing the synchronized solution about this frequency. As the amplitude of the components in $\bar{P}$ increases, the approximated expression (4) becomes invalid. However, taking into account the evolution of the solution curves in sinusoidally injection-locked oscillators [6], one can expect the closed curves to evolve into open resonance curves. Considering the joint effect of all the sources $u_r(t)$, there will be resonance curves in the $(\Delta V_{ik}, \omega_p)$ space centered around all the ω_p values fulfilling $r\omega_p = m\omega_0$.

The above theoretical analysis explains the behavior observed in Fig. 1a. The resonance curves are centered about $\omega_p = m\omega_0/r$. On the right-hand side of Fig. 1a, for $m = 1$ and when decreasing ω_p, the positive integer r increases in one at each resonance, starting from $r = 42$ at the first resonance. Therefore, the distance between the maxima decreases as $\omega_0/[(r+1)r]$. For high ω_p, open synchronization curves are obtained, which become narrower when reducing ω_p. For low ω_p, the curves start to exhibit turning points and finally break into a closed- and an open curve of lower amplitude. This is why the lower frequency resonances are incomplete in Fig. 1a.

The results of time-domain integration have been superimposed with dots in Fig. 1a. For high ω_p, the curves obtained with HB and time-domain analysis are fully overlapped. For lower ω_p there is disagreement near the minima. This is due to the instability of the injection-locked solution. In fact, when decreasing ω_p, frequency divisions by two and other phenomena are observed.

The stability of the periodic steady-state regime at ω_p, has been analyzed applying pole-zero identification along the solution curve in Fig. 1a. This technique is based on the calculation of a closed-loop transfer function associated to the circuit linearization about the periodic regime at ω_p, performed with the conversion-matrix approach [6]. The variation of the real part of the poles in three different intervals is shown in Fig. 2. For $f_p > 29.2$ MHz, the analysis shows that the real part of the dominant poles approach zero at the minima of the curve in Fig. 1 but does not become positive, so the circuit is always stable. In fact the frequency of the poles with the largest real part agrees with $\omega_p/2$, that is, they have the form $\sigma \pm j\omega_p/2$. About the minima, there is a second pair of poles $\sigma' \pm j\omega_p/2$. When either decreasing or increasing ω_p, the two pairs of poles at $\omega_p/2$ merge into two complex conjugate poles $\sigma \pm j\omega_a$, such that ω_a equals $\omega_p/2$ at the merging point. From the merging point, ω_a becomes (continuously) incommensurable with ω_p and there is only one curve in the representation of Fig. 2, since the two poles $\sigma \pm j\omega_a$ have the same real part. The described transformation preserves the system dimension, since, according to Floquet theory [7], each pair of poles $\sigma \pm j\omega_p/2$ corresponds to a single real Floquet multiplier and the complex-conjugate poles at an incommensurate frequency correspond to a pair of complex-conjugate multipliers.

For $f_p < 29.2$ MHz, the poles cross to the right hand side of the complex plane in the low amplitude sections of the curve in Fig. 1a. In the interval $23.8\text{ MHz} < f_p < 29.2$ MHz, the poles that cross to the RHP have the subharmonic frequency $\omega_p/2$, because the merging into complex-conjugate poles takes place on the left-hand side of the complex plane. For $f_p < 23.8$ MHz, the frequency of the poles that cross to the RHP is incommensurable with ω_p. This is because the merging of the subharmonic poles takes place on the RHP. Therefore, there are two different types of bifurcation [4-5,7] delimiting the stable synchronization ranges. In the interval $23.8\text{ MHz} < f_p < 29.2$ MHz, the ranges will be delimited by flip bifurcations, at which a division by two of the input frequency ω_p takes place. For $f_p < 23.8$ MHz, the stable synchronization ranges will be delimited by Hopf bifurcations, from which the solution will have two fundamental frequencies: ω_p and an incommensurable frequency ω_a. It should be noted that the stable regions decrease substantially when reducing ω_p.

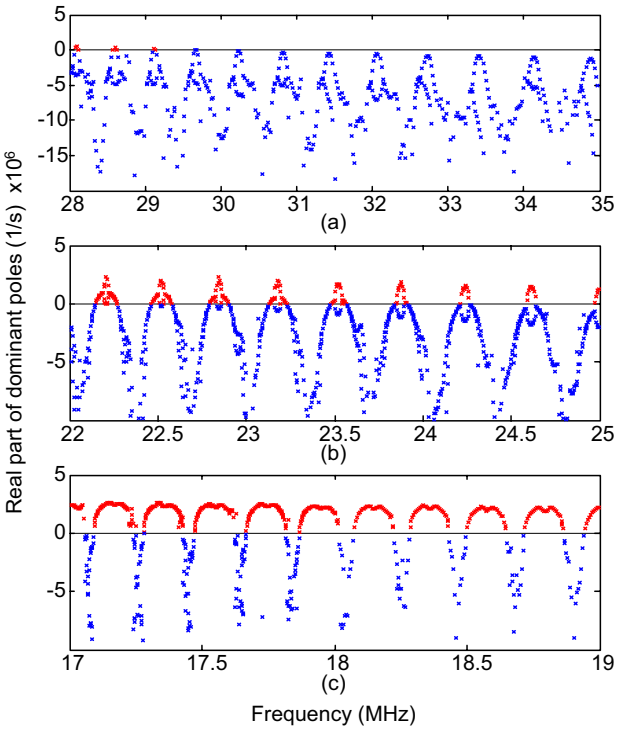

Fig. 2 Stability analysis performed along the solution curve in Fig. 1a. The real part of the poles has been represented versus ω_p. (a) 28 – 35 MHz. (b) 22 – 25 MHz. (c) 17 – 19 MHz.

The behavior is analogous to that obtained in an oscillator synchronized at the fundamental frequency. For sufficiently large input power, the solution curve is open [4], with instability occurring in the lower amplitude ranges, due to the increase of the negative resistance. In the upper-frequency range of Fig.1, the influence of the multi-harmonic input signal pushes the imaginary part of the poles to $\omega_p/2$ and divisions by two are observed. For low input frequencies, the synchronization regions become negligible and the circuit will generally behave in quasi-periodic regime. Another essential difference with respect to the behavior of sinusoidally injection-locked oscillators is the possibility to pass from one resonance to another without loss of stability. This is observed in Fig. 2 for $f_p > 29.2$ MHz.

III. Application to a Bipolar-Based Oscillator

The generality of the synchronized behavior and stability properties studied in the previous subsection has been verified through application to other oscillators, based on bipolar

transistors. Here the results obtained with the circuit in Fig. 3, based on the transistor BFP405, will be presented. In the absence of an input signal, the circuit oscillates at the free-running frequency $f_o = 5.7$ GHz. Fig. 4 shows the synchronization curve obtained for N = 14 harmonics in p(t). The curve has been obtained tracing the maxima of the steady state waveform versus the pulse frequency, using time-domain integration. In some frequency intervals, two or more discrete points are represented, which is due to the fact that the waveform exhibits two or more maxima. This is because the solution is no longer periodic at the input frequency ω_p. In the case of a period doubling, two points are obtained, whereas in the case of a quasi-periodic solution, a distribution of points is obtained. This result is in agreement with the stability analysis of Fig. 2, which shows that instability occurs about the minima of the solution curve. Fig. 5 shows the waveforms obtained for two different values of the pulse frequency $f_p = 78.6$ MHz (regular behavior) and $f_p = 78.8$ MHz (frequency division by two). The spectra measured for $f_p = 35$ MHz (frequency-division by 2) and $f_p = 31$ MHz are shown in Fig. 6.

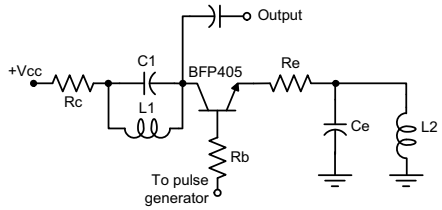

Fig. 3 Schematic of the bipolar-based oscillator.

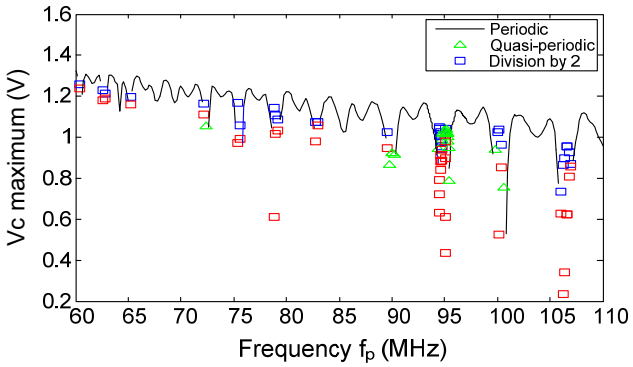

Fig. 4 Multi-resonance behavior of the oscillator in Fig. 3, with free-running frequency f_0= 5.7 GHz.

IV. Conclusion

The occurrence of ultra-subharmonic synchronization in oscillators driven with multi-harmonic signals has been demonstrated. The multi-resonance behavior versus the input frequency has been analyzed in depth, studying the bifurcation phenomena that delimit the stable synchronization bands. The analysis has been illustrated through application to an oscillator at 5.7 GHz.

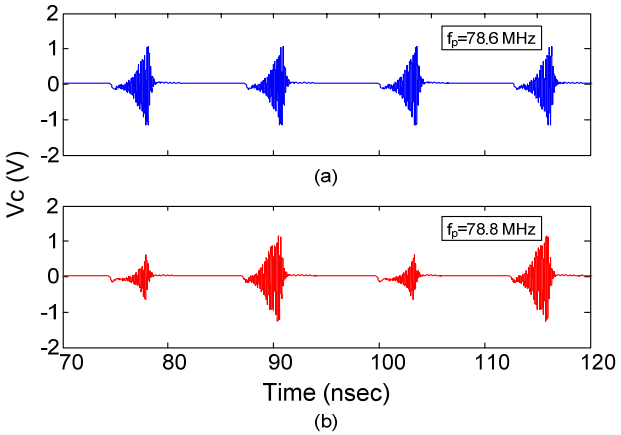

Fig. 5 Steady-state waveforms of the oscillator in Fig. 3 for two different values of ω_p.

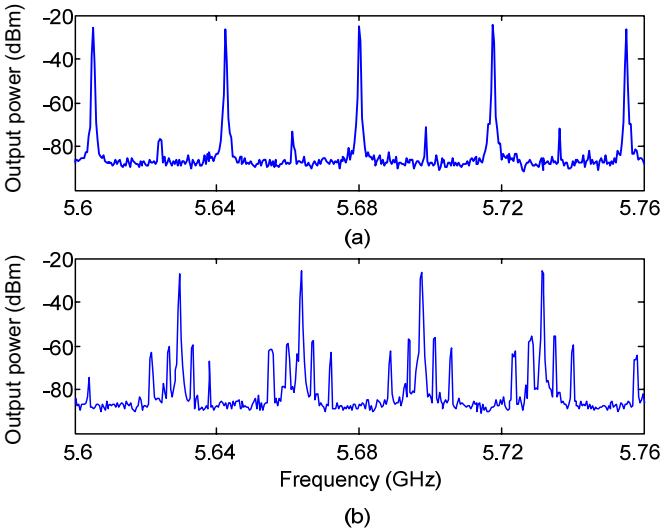

Fig. 6 Measured spectra of the oscillator in Fig. 3 in the unstable behavior regions. (a) Frequency division by 2 for f_p=35 MHz. (b) Quasi-periodic behavior for f_p=31 MHz.

Acknowledgment

This work has been supported by the Spanish Government under contract TEC2011-29264-C03-01.

References

[1] N. Deparis, C. Loyez, N. Rolland, P.A. Rolland, "UWB in millimetrc wave band with pulsed ILO", *IEEE Trans. Circuits and Systems II,* vol. 55, no. 4, pp. 339-343.

[2] N. Deparis, A. Siligaris, P. Vincent, N. Rolland, "A 2 pJ/bit pulsed ILO UWB transmitter at 60 GHz in 65-nm CMOS-SOI" *IEEE International Conference on Ultrawideband,* Oct. 2009, pp. 113-117.

[3] F. Ramirez, A. Suarez, S. Sancho, E. Fernandez, "Nonlinear analysis of pulsed injection-locked oscillators," IEEE MTT-S Int. Microwave Symp., Montreal, Canada, June, 2012.

[4] A. Suárez, Analysis and design of autonomous microwave circuits, IEEE-Wiley, 2009.

[5] S. Wiggins, *Introduction to applied nonlinear dynamical systems* and chaos, Springer, 1990.

[6] J. Jugo, J. Portilla, A. Anakabe, A. Suarez, J. M. Collantes, "Closed-loop stability analysis of microwave amplifiers," *IEE Electronics Letters*, Vol. 37, No. 4, pp. 226-228, Feb. 2001.

[7] S. Parker, L. Chua, Practical Numerical Algorithms for Chaotic Systems, Springer, 1989.